THE JOURNAL OF PHYSICAL CHEMISTRY C

Article

pubs.acs.org/JPCC

Water-Free Proton Conduction in Hexakis(*p*-Phosphonatophenyl)benzene Nanochannels

Christoph Wehmeyer,[†,‡] Manuel Schrader,[§] Denis Andrienko,[§] and Daniel Sebastiani*[,‡]

[†]Dahlem Center for Complex Quantum Systems, Freie Universität Berlin, Arnimeallee 14, 14195 Berlin, Germany

[‡]Institute of Chemistry, Martin-Luther-Universität Halle-Wittenberg, von-Danckelmann-Platz 4, 06120 Halle, Germany

[§]Max Planck Institute for Polymer Research, Ackermannweg 10, 55128 Mainz, Germany

Supporting Information

ABSTRACT: We elucidate the proton conduction mechanism in self-assembling stacks of phosphonic-acid-functionalized molecules (hexakis(*p*-phosphonatophenyl)benzene) at different temperatures (400−600 K) and at zero humidity conditions. We employ first-principles molecular dynamics simulations in combination with large-scale force-field simulations, forming a specific arrangement of the molecules in the columnar stacks. This arrangement leaves space for quasi-one-dimensional hydrogen bond nanowires along which protons are transported. We observe spontaneous autodissociation of the phosphonic acid groups, leading to proton displacements of up to 10 Å along the nanowires. Our simulations show that there is a fast (200 fs) and a slow (3−12 ps) component in the dynamics of the hydrogen bond network, corresponding to orientation fluctuations of the hydrogen bonds and persistent long-range proton transport, respectively. Our results support the hypothesis that significant proton conduction is possible in this compound at fully dehydrated conditions and at high temperatures. In such circumstances, the material may outperform the common Nafion polymer as membrane materials for proton exchange fuel cells.

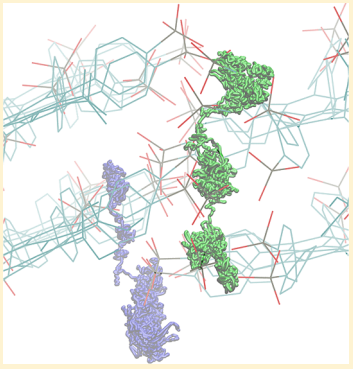

1. INTRODUCTION

Hydrogen has a potential to become an alternative energy carrier, radically changing our lifestyles and global economies.[1] As any energy carrier, hydrogen has to be produced, stored, and converted into (in this case) electrical energy. The conversion is normally performed in a hydrogen fuel cell, the core component of which is a proton exchange membrane. This membrane has to be chemically stable, durable, and proton conducting.[2] Nafion is a state-of-art material for such membranes.[3,4] Its remarkable proton conductivity relies on the formation of hydrophilic domains forming a network of water channels, where efficient proton transfer takes place, similar to pure water.[5] This, however, limits the membrane operation temperature by the boiling point of water, imposing costly requirements on catalysts and hydrogen purity.

To extend the operational temperature range, one can exchange water channels with proton-conductive liquids with a higher boiling point, e.g., imidazole derivatives,[6] or synthesize new polymeric materials with intrinsic proton conductivity,[7] for example, by using functionalized phosphonic acid groups.[8−11] The concentration of these groups should, however, be high enough to ensure efficient proton transport.[12−15] Finally, the spatial arrangement of these functional groups should form percolating pathways for protons moving through the membrane. Both issues can be addressed by using self-organizing supramolecular assemblies, such as recently proposed organic phosphonated molecules.[16−19] Some of them, such as tris(*p*-phosphonatophenyl)benzene (*p*-3 PA-HPB) and hexakis(*p*-phosphonatophenyl)benzene (*p*-6 PA-HPB, see Figure 1), form columnar structures with molecules stacked on top of each other (see Figure 2), as has been demonstrated by XRD measurements. While *p*-3 PA-HPB decomposes at 120 °C, *p*-6

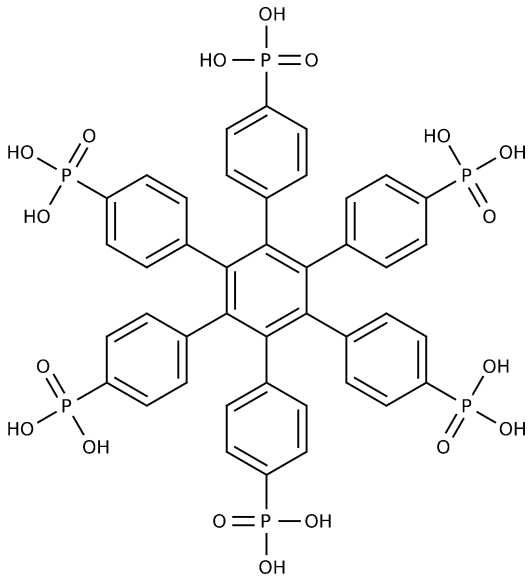

Figure 1. Molecular structure of *p*-6 PA-HPB.

Received: April 9, 2013
Revised: May 21, 2013
Published: May 22, 2013

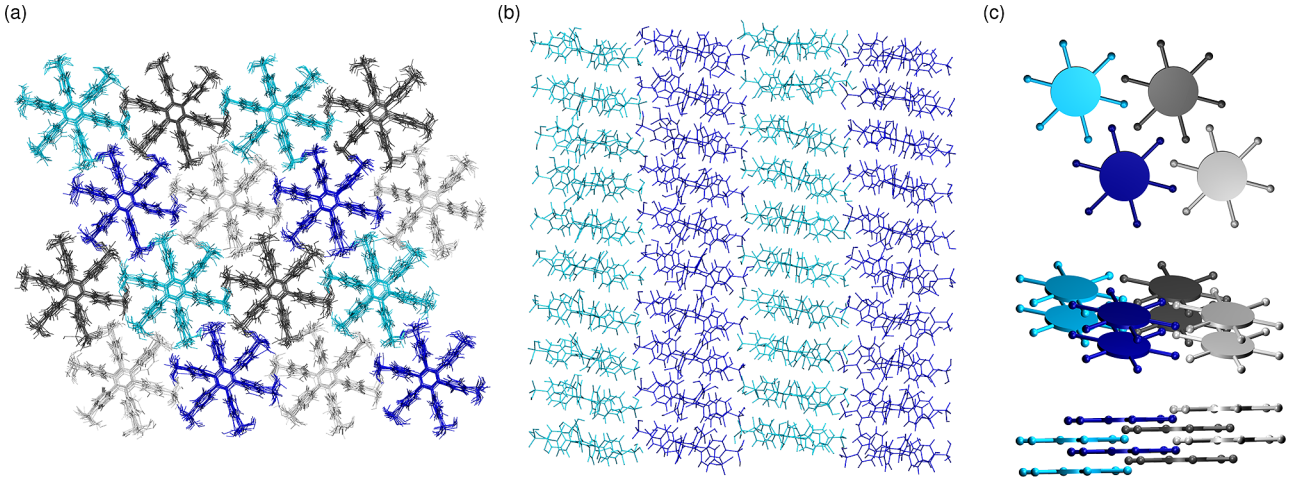

Figure 2. (a, b) Simulation snapshot of 4 × 4 columns arranged on a hexagonal lattice with ten *p*-6 PA-HPB molecules in each column. The snapshot is taken after 10 ns equilibration. (c) Schematic mutual arrangement of the *p*-6 PA-HPB molecules in the columnar stacks found after extensive equilibration of the supramolecular arrangement.

PA-HPB remains stable far beyond, and its proton conductivity exceeds that of Nafion at 160 °C; the conductivity of Nafion decreases rapidly due to loss of water in the water channels.[20−22]

In addition to the poor understanding of the microscopic mechanism of proton transfer and transport in such materials, the formulation of qualitative structure−property relations, that is, links between the chemical structure and the (macroscopic) value of proton conductivity, is a formidable task because of difficulties in characterizing experimentally and predicting theoretically their (mesoscopic) molecular ordering. In this work, we use a multiscale simulation approach in order to formulate such structure−property relations for *p*-6 PA-HPB, the chemical structure of which is shown in Figure 1.

Considerable efforts are reported in recent literature for the rational design of hydrogen-bonded molecular crystals based on this type of compound.[23] Although the vision behind this is the design of water-free proton conductors, it is established that really crystalline domains are not always optimal for proton conduction,[24,25] and that residual water molecules indeed play an important role in the conduction process.[26−29]

A complementary topic of high relevance is the determination of the impact of the pK_a value of the system[30] and its interaction with the topology of the hydrogen bond network.[31] In the case of self-assembled *p*-6 PA-HPB aggregates, the isotropic character of compounds such as Nafion is lost; instead, a preferred direction exists along the columnar stacks, in analogy to biomolecular systems such as one-dimensional ion-conducting channels in proteins.[32]

It has recently been suggested that even purely coordination-type compounds can support long-range proton transport if adequate proton acceptor/donor groups are included.[33] Similarly, suitably filled MOFs have been shown to be capable of proton conduction,[34] even under very low humidity conditions.[35]

In the present work, we investigate the structural packing motif of supramolecular assemblies of *p*-6 PA-HPB and the structural and dynamical properties of the emerging hydrogen bond network by means of classical and quantum mechanical molecular dynamics simulations. These simulations help to understand the microscopic proton conduction mechanism under dry conditions that has been measured experimentally.

2. RESULTS AND DISCUSSION

2.1. Molecular Dynamics Simulations. In order to better understand the packing motifs of *p*-6PA-HPB, we first performed classical molecular dynamics (MD) simulations of its columnar arrangement using an OPLS all-atom force-field.[36] The force-field parameters are available in the Supporting Information. The starting configuration was inspired by the interpretation of X-ray diffraction measurements:[18,19] 16 columns were arranged on a 4 × 4 hexagonal lattice, with ten *p*-6PA-HPB molecules in each column. After a 10 ns MD run in an *NPT* ensemble (T = 350 K, P = 1 atm) using the Berendsen barostat[37] and the canonical velocity rescaling thermostat,[38] the molecules in the columns rearrange as shown in Figure 2a,b.

Already a visual inspection of the hexagonal stacks indicates that the computationally observed supramolecular packing yields a highly optimized space-filling arrangement. The phosphonic acid groups are located in positions that allow a particularly high degree of intercolumnar hydrogen bonding. The stacking distance of roughly 6 Å does not, however, enable direct intracolumnar hydrogen bonding.

From an equilibrated supercell, we have devised a model of the supramolecular arrangement, which is shown in Figure 2c. The molecular stacks are arranged on a hexagonal lattice with neighboring columns shifted along the columnar axis (this increases the density of intercolumnar hydrogen bonds). Note that the conjugated cores of *p*-6 PA-HPB are slightly tilted with respect to the columnar axis. This small tilt is not accounted for in the model arrangement; that is, we assume that the columnar axes are perpendicular to the conjugated π-systems of the *p*-6 PA-HPB molecules.

We used a representative packing motif that has been extracted from the classical MD trajectory as starting point for our *ab initio* MD simulations. The latter were performed on the level of Kohn−Sham density functional theory[39−41] (DFT) using the electronic structure code CP2K[42−45] with a computational setup according to Table 1.

Our system consists of eight *p*-6 PA-HPB molecules in an orthorhombic, periodic box of volume V = 29.122 × 25.354 × 12.363 Å^3. We have adopted zero humidity conditions; that is, no explicit water molecules are present in our setup. The simulations were carried out at temperatures T = 400, 500, and 600 K. Experimental evidence suggested that *p*-6 PA-HPB is chemically

dx.doi.org/10.1021/jp4035024 | J. Phys. Chem. C 2013, 117, 12366−12372

Table 1. Computational Setup of the *ab Initio* Molecular Dynamics Simulations

functional	BLYP[46,47]
basis set	TZVP-GTH (GPW)[48,49]
pseudopotential	GTH[50,51]
AIMD time step	0.4 fs
dispersion correction	Grimme[52]
thermostat type	CSVR[38]
thermostat time constant	400 fs
AIMD equilibration time	10 ps
AIMD production time	30 ps

stable at intermediate temperatures, shows self-condensation of the acidic groups around 550 K, and shows decomposition of the hydrophobic core above 720 K.[18,19]

2.2. Radial Distribution Functions. We have computed radial distribution functions (RDFs) for hydrogen−oxygen and phosphorus−phosphorus at 400 K, 500 K, and 600 K; the RDFs were averaged over 30 ps each.

The RDF for hydrogen−oxygen (g_{HO}) is shown in Figure 3. The general shape is nearly identical for all temperatures. We

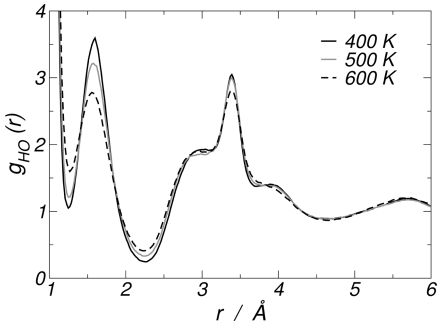

Figure 3. Radial distribution function $g_{HO}(r)$ for hydrogen−oxygen at 400 K (black/full), 500 K (gray/full), and 600 K (black/dashed).

observe that the amplitude of the hydrogen bonding peak at 1.5−1.7 Å is somewhat reduced (from 3.6 to 3.2 and 2.9) upon raising the temperature from 400 to 500 and 600 K. Further, we find an additional broad peak starting at an H−O distance of 2.9 Å, which ends in a more narrow peak between 3.2 and 3.7 Å. This peak is perfectly identical for all temperatures and has an amplitude of 3 for 400 and 500 K and a reduced amplitude of 2.9 at 600 K.

We computed the average number of oxygen atoms under the broad peak and the more narrow peak and found n_{broad} = 7 oxygens in the range 2.3−4.3 Å and n_{narrow} = 2 oxygens in the range 3.25−3.6 Å. These observations can be explained as follows: every hydrogen atom is part of one acidic group and has two more acidic groups from adjacent stacks in its close proximity, which adds up to nine oxygen atoms in this area. The hydrogen is covalently bonded to one oxygen of its own acidic group and forms a hydrogen bond with an oxygen of an adjacent acidic group; this explains why we find n_{broad} = 7 oxygens under the broad peak. Further, we found that the n_{narrow} = 2 oxygens under the narrow peak split up into one oxygen from the own acidic group of the hydrogen and one oxygen from the acidic group to which the hydrogen is connected via its hydrogen bond.

For the analysis of the structural relation between phosphorus atoms, we use a modified definition of the radial distribution function that takes into account the number of hydrogen bonds that connect the acidic groups. Figure 4a−c shows the RDFs for

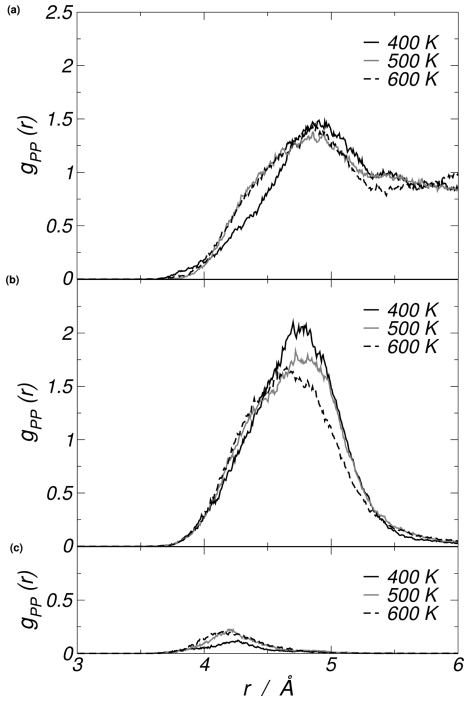

Figure 4. (a−c) Partial phosphorus−phosphorus radial distribution functions $g_{PP}(r)$ at 400 K (black/full), 500 K (gray/full), and 600 K (black/dashed) for phosphonic acids with no mutual hydrogen bond (a), those with one single hydrogen bond between them (b), and those with doubly hydrogen-bonded phosphonic acid pairs (c).

phosphorus−phosphorus at 400, 500, and 600 K. In particular in Figure 4, panel a shows the non-hydrogen-bonded contribution, panel b the single-bonded contribution, and panel c the double-bonded contribution to the total $g_{PP}(r)$. Further, we fit each curve with a single Gaussian,

$$f_g(r) = a \exp\left(-\frac{(r-\mu)^2}{2\sigma^2}\right) \quad (1)$$

to determine the amplitudes a, the centers of the peaks μ, and the standard deviations σ. With these parameters, we can compute the coordination numbers n of the individual features:

$$n = 4\pi \int_0^\infty \mathrm{d}r\, r^2 f_g(r)\rho \quad (2)$$

where ρ is the average phosphorus density in our simulation box. The resulting parameters are shown in Table 2.

We find that each acidic group has four different groups with a distance of 4.8 ± 0.5 Å between their phosphorus atoms and shares hydrogen bonds with two of its neigbors. Occasionally,

Table 2. Centers and Standard Deviations, $\mu \pm \sigma$, of Gaussian Fits $f_g(r)$ of the $g_{PP}(r)$ According to Eq 1 and Coordination Numbers n Computed from Eq 2

	400 K	500 K	600 K
nonbonded [Å]	4.9 ± 0.4	4.8 ± 0.5	4.8 ± 0.4
single-bonded [Å]	4.7 ± 0.4	4.7 ± 0.4	4.7 ± 0.4
double-bonded [Å]	4.2 ± 0.2	4.2 ± 0.2	4.2 ± 0.2
nonbonded [1]	2.0	2.0	2.0
single-bonded [1]	2.6	2.5	2.2
double-bonded [1]	0.1	0.1	0.1
coordination [1]	4.7	4.6	4.3

dx.doi.org/10.1021/jp4035024 | J. Phys. Chem. C 2013, 117, 12366−12372

two acidic groups share two hydrogen bonds, which coincides with a much shorter P−P distance of 4.2 ± 0.2 Å. The average coordination of the phosporus atoms is 4.7 at 400 K and decreases to 4.6 and 4.3 when the temperature is raised to 500 and 600 K. A frame-wise inspection of the MD trajectories yields that the hydrogen bonding occurs in 99.98% of all cases on the intermolecular level.

2.3. Hydrogen Bond Network. In order to analyze the characteristic time scales of the hydrogen bond network, we define a hydrogen bond correlation function via[27,29,53]

$$\eta_{\mathrm{hbn}}(t) = \langle \sum_k \tilde{\delta}_{H_k^{\mathrm{hbn}}(t+t_0),H_k^{\mathrm{hbn}}(t_0)} \rangle_{t_0} \tag{3}$$

Here, $\tilde{\delta}_{H_k^{\mathrm{hbn}}(t+t_0),H_k^{\mathrm{hbn}}(t_0)} = 1$ if the acidic proton k forms at both times t and $t + t_0$ a hydrogen bond with the same pair of acceptor oxygens and 0 otherwise. To be counted as a hydrogen bond, the proton must be covalently bonded to the nearest of the oxygens ($r_{\mathrm{OH}} < 1.3$ Å), the distance between the proton and the other oxygen must be $\tilde{r}_{\mathrm{OH}} < 2.2$ Å, and the angle between the covalent O−H axis and the hydrogen-bonded H−O axis must be $\alpha < 60°$. Hence, the hydrogen bond correlation function $\eta_{\mathrm{hbn}}(t)$ counts the number of hydrogen bonds at time t that have already existed at the initial time t_0. Figure 5 shows the hydrogen bond correlation function for different temperatures.

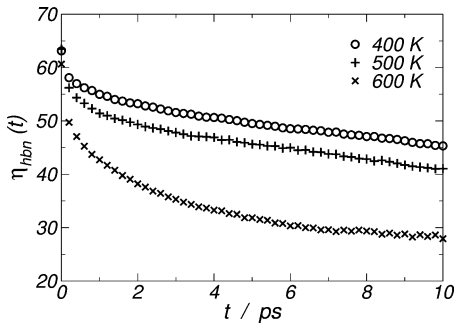

Figure 5. The hydrogen bond correlation function $\eta_{\mathrm{hbn}}(t)$ according to eq 3 characterizes the evolution of the local hydrogen bond network.

We fit the bond correlation functions with a bimodal exponential decay and a constant term:

$$f_\eta(t) = a_0 + \sum_{i=1}^{2} a_i \, \mathrm{e}^{-t/\tau_i} \tag{4}$$

The resulting parameters of this fit function are shown in Table 3.

We observe that the decay of the HBN is governed by two distinct time scales: the fast process on a time scale of roughly $\tau_{\mathrm{fast}} \leq 0.3$ ps and the comparably slow process on a time scale of $\tau_{\mathrm{slow}} \approx 3-12$ ps.

Table 3. Parameters for a Fit with Eq 4 of the Hydrogen Bond Correlation Function $\eta_{hbn}(t)$

parameter	400 K	500 K	600 K
a_2 (fast) [1]	6.5	10.5	11.9
τ_2 (fast) [ps]	0.2	0.3	0.1
a_1 (slow) [1]	15.7	20.0	21.0
τ_1 (slow) [ps]	8.5	11.7	3.0
a_0 (asymptotic) [1]	40.9	32.7	27.7

The fast process corresponds to the reversible forth-and-back switching of a hydrogen bond between two acceptor oxygens from neighboring acid groups. The slow process is caused by rotational motion of the individual phosphonic groups.

2.4. Proton Mobility. The motion of protons through the slab of *p*-6 PA-HPB molecules is intrinsically connected to the breaking and formation of covalent O−H bonds in the phosphonic acids. To estimate the amount of broken bonds over time, we defined a covalent bond correlation function similar to eq 3,

$$\eta_{\mathrm{cov}}(t) = \langle \sum_k \tilde{\delta}_{H_k^{\mathrm{cov}}(t+t_0),H_k^{\mathrm{cov}}(t_0)} \rangle_{t_0} \tag{5}$$

where, $\tilde{\delta}_{H_k^{\mathrm{cov}}(t+t_0),H_k^{\mathrm{cov}}(t_0)} = 1$ if the acidic proton k is at both times covalently bonded to the same oxygen and 0 otherwise. To be counted as a covalent bonded pair, the O−H distance, r_{OH}, must be $r_{\mathrm{OH}} < 1.3$ Å. Thus, $\eta_{\mathrm{cov}}(t)$ is the average number of covalent O−H bonds in the original HBN (at time t_0) that are still conserved after simulation time t.

The covalent bond correlation function, $\eta_{\mathrm{cov}}(t)$, is shown in Figure 6 (top). We observe that 5−10 O−H bonds are lost within 1 ps and that the decay reaches a plateau with a total loss of 15−30 covalent O−H bonds.

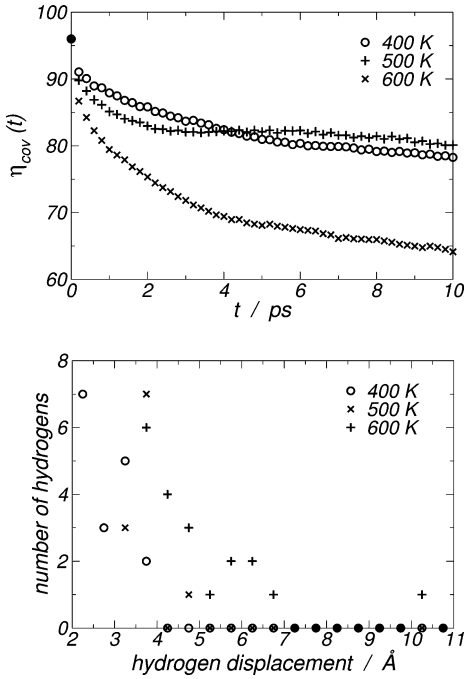

Figure 6. The covalent O−H bond correlation function, $\eta_{\mathrm{cov}}(t)$, according to eq 5 (top) and the displacement of the acidic hydrogen atoms after $\Delta t = 30$ ps (bottom) at 400 K (●), 500 K (×), and 600 K (+).

To further gauge the mobility of the acidic protons, we computed the distribution of the total proton displacements after 30 ps, which is shown in Figure 6 (bottom). We observe that for all temperatures, most of the 96 acidic protons in the system did move less than 2 Å, which roughly corresponds to the distance of a transfer from one phosphonic acid group to one of its direct neighbors, followed by a local reorientation. In the simulation at $T = 400$ K, no proton diffuses further than 4 Å, and at $T = 500$ K, a single proton reaches a displacement of 5 Å. However, the MD simulation at $T = 600$ K yields six proton translations of about 6 Å

dx.doi.org/10.1021/jp4035024 | J. Phys. Chem. C 2013, 117, 12366−12372

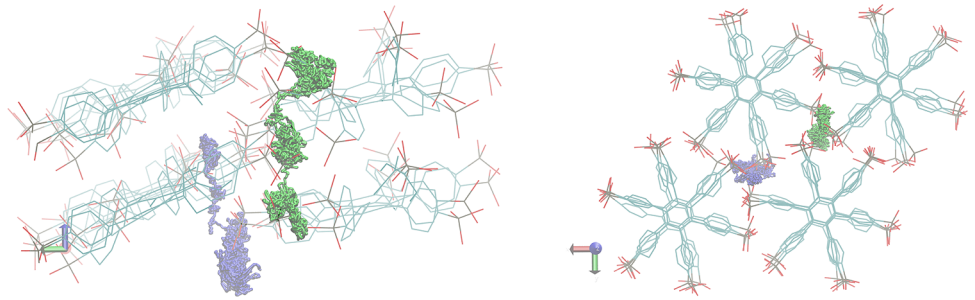

Figure 7. Pathways (green and blue) of two highly mobile protons parallel to the columnar axis. The path corresponds to a total travel time of 30 ps at 600 K. Superimposed molecular structures are taken from snapshots at 0 and 30 ps.

and one of 10 Å. While these numbers are certainly not converged in the statistical sense, they nevertheless illustrate the onset of fast long-range diffusion processes at increased temperatures.

It should be mentioned that this diffusive transport would correspond to a remarkably high current density on the order of 2 A/mm^2, roughly estimated from the average displacement of the protons that travel further than 5 Å and under the assumption that all protons move in the same direction.

We tracked the movement of those protons that autodissociate and diffuse over larger distances in the trajectory at 600 K. We observe that the protons travel within the interstice where three columns adjoin each other and that it is parallel to the columnar axis. This situation is sketched for two protons in Figure 7.

3. CONCLUSIONS

We have modeled the local packing structure of self-assembling disk-shaped hexakis(*p*-phosphonatophenyl)benzene molecules in a hexagonal pattern of supramolecular stacks in fully dehydrated conditions. The packing gives rise to a tight interstack hydrogen bond network. Our first-principles molecular dynamics simulations show that there is a specific region at the geometric centers of every triplet of stacks, which features quasi-one-dimensional proton conducting channels. Our simulations detect spontaneous autodissociation of the phosphonic acid groups, leading to a considerable charge carrier diffusion mainly parallel to the stacks. Remarkably, both the autodissociation and the proton diffusion are observed in the absence of any water molecule. This feeds hope that high-temperature low-humindity proton exchange membrane materials are getting in reach, which would significantly enhance the efficiency of the corresponding hydrogen fuel cell systems.

Our structural investigation shows that at all temperatures the typical phosphonic acid group is hydrogen-bonded to two of the four adjacent acid groups from two *different* stacks; intracolumnar hydrogen bonding was not observed. This represents clear evidence for a properly percolating hydrogen bond network in the *p*-6 PA-HPB stacks, which will support sustained long-range proton conduction.

The duration of our *ab initio* MD simulations is presently still too short to cover the time scale required for a quantitative determination of proton diffusion. Nevertheless, the trend in the maximum displacement (as reported in Figure 6, bottom) is obvious: the number of protons with displacements larger than 3 Å is seven (at T = 400 K), eleven (at T = 500 K), and more than twenty (at T = 600 K). In the latter case, around 20% of all acidic protons travel this far within our 30 ps simulation. This illustrates the high sensitivity of the proton mobility on temperature and confirms that compounds based on phosphonic acid groups represent indeed a highly promising candidate for "dry" fuel cell membrane materials.

■ ASSOCIATED CONTENT

Ⓢ Supporting Information

Parameters of the all-atom force-field. This material is available free of charge via the Internet at http://pubs.acs.org.

■ AUTHOR INFORMATION

Corresponding Author

*E-mail: daniel.sebastiani@chemie.uni-halle.de.

Notes

The authors declare no competing financial interest.

■ ACKNOWLEDGMENTS

This work has been supported by the German Research Foundation (DFG) under Grant SE 1008/6. M.S. was partially supported by the DFG International Research Training Group 1404. Computing infrastructure was provided by the Northern German Supercomputing Alliance (HLRN) under Grant HLRN/bec00082.

■ REFERENCES

(1) Crabtree, G. W.; Dresselhaus, M. S.; Buchanan, M. V. The Hydrogen Economy. *Phys. Today* **2004**, *57*, 39−44.

(2) Steele, B. C.; Heinzel, A. Materials for Fuel-Cell Technologies. *Nature* **2001**, *414*, 345−352.

(3) Paddison, S. J.; Paul, R. The Nature of Proton Transport in Fully Hydrated Nafion. *Phys. Chem. Chem. Phys.* **2002**, *4*, 1158−1163.

(4) Rozière, J.; Jones, D. J. Non-Fluorinated Polymer Materials for Proton Exchange Membrane Fuel Cells. *Annu. Rev. Mater. Res.* **2003**, *33*, 503−555.

(5) Tuckerman, M. E.; Marx, D.; Klein, M. L.; Parrinello, M. On the Quantum Nature of the Shared Proton in Hydrogen Bonds. *Science* **1997**, *275*, 817−820.

(6) Kreuer, K.-D.; Paddison, S. J.; Spohr, E.; Schuster, M. F. H. Transport in Proton Conductors for Fuel-Cell Applications: Simulations, Elementary Reactions, and Phenomenology. *Chem. Rev.* **2004**, *104*, 4637−4678.

(7) Roy, S.; Ataol, T. M.; Müller-Plathe, F. Molecular Dynamics Simulations of Heptyl Phosphonic Acid: A Potential Polymer Component for Fuel Cell Polymer Membrane. *J. Phys. Chem. B* **2008**, *112*, 7403−7409.

(8) Schuster, M.; Rager, T.; Noda, A.; Kreuer, K. D.; Maier, J. About the Choice of the Protogenic Group in PEM Separator Materials for Intermediate Temperature, Low Humidity Operation: A Critical Comparison of Sulfonic Acid, Phosphonic Acid and Imidazole Functionalized Model Compounds. *Fuel Cells* **2005**, *5*, 355−365.

(9) Joswig, J.-O.; Seifert, G. Aspects of the Proton Transfer in Liquid Phosphonic Acid. *J. Phys. Chem. B* **2009**, *113*, 8475−8480.

(10) Vilčiauskas, L.; Paddison, S. J.; Kreuer, K.-D. Ab Initio Modeling of Proton Transfer in Phosphoric Acid Clusters. *J. Phys. Chem. A* **2009**, *113*, 9193−9201.
(11) Vilčiauskas, L.; Tuckerman, M. E.; Bester, G.; Paddison, S. J.; Kreuer, K.-D. The Mechanism of Proton Conduction in Phosphoric Acid. *Nat. Chem.* **2012**, *4*, 461−466.
(12) Steininger, H.; Schuster, M.; Kreuer, K.-D.; Kaltbeitzel, A.; Bingöl, B.; Meyer, W. H.; Schauff, S.; Brunklaus, G.; Maier, J.; Spiess, H. W. Intermediate Temperature Proton Conductors for PEM Fuel Cells based on Phosphonic Acid as Protogenic Group: A Progress Report. *Phys. Chem. Chem. Phys.* **2007**, *9*, 1764−1773.
(13) Kreuer, K.-D.; Wohlfarth, A. Limits of Proton Conductivity. *Angew. Chem., Int. Ed.* **2012**, *51*, 10454−10456.
(14) Vuilleumier, R.; Borgis, D. Proton Conduction: Hopping along Hydrogen Bonds. *Nat. Chem.* **2012**, *4*, 432−433.
(15) Kobayashi, K.; Shirasaka, T.; Sato, A.; Horn, E.; Furukawa, N. Self-Assembly of a Radially Functionalized Hexagonal Molecule: Hexakis(4-hydroxyphenyl)benzene. *Angew. Chem., Int. Ed.* **1999**, *38*, 3483−3486.
(16) Jones, K. M. E.; Mahmoudkhani, A. H.; Chandler, B. D.; Shimizu, G. K. H. An Adamantane-based Tetraphosphonic Acid That Forms an Open Diamondoid Net via a Hydrogen-Bonded Phosphonic Acid-Water Cluster. *CrystEngComm* **2006**, *8*, 303−305.
(17) Beckmann, J.; Rüttinger, R.; Schwich, T. 1,3,5-Benzene-tri-p-Phenylphosphonic Acid. A New Building Block in Supramolecular Chemistry. *Cryst. Growth Des.* **2008**, *8*, 3271−3276.
(18) Jiménez-García, L.; Kaltbeitzel, A.; Pisula, W.; Gutmann, J. S.; Klapper, M.; Müllen, K. Phosphonated Hexaphenylbenzene: A Crystalline Proton Conductor. *Angew. Chem., Int. Ed.* **2009**, *48*, 9951−9953.
(19) Jiménez-García, L.; Kaltbeitzel, A.; Enkelmann, V.; Gutmann, J. S.; Klapper, M.; Müllen, K. Organic Proton-Conducting Molecules as Solid-State Separator Materials for Fuel Cell Applications. *Adv. Funct. Mater.* **2011**, *21*, 2216−2224.
(20) Ye, G.; Janzen, N.; Goward, G. R. Solid-State NMR Study of Two Classic Proton Conducting Polymers: Nafion and Sulfonated Poly(ether ether ketone)s. *Macromolecules* **2006**, *39*, 3283−3290.
(21) Ye, G.; Hayden, C. A.; Goward, G. R. Proton Dynamics of Nafion and Nafion/SiO_2 Composites by Solid State NMR and Pulse Field Gradient NMR. *Macromolecules* **2007**, *40*, 1529−1537.
(22) Yu, T. H.; Sha, Y.; Liu, W.-G.; Merinov, B. V.; Shirvanian, P.; Goddard, W. A., III Mechanism for Degradation of Nafion in PEM Fuel Cells from Quantum Mechanics Calculations. *J. Am. Chem. Soc.* **2011**, *133*, 19857−19863.
(23) Maly, K. E.; Gagnon, E.; Maris, T.; Wuest, J. D. Engineering Hydrogen-Bonded Molecular Crystals built from Derivatives of Hexaphenylbenzene and Related Compounds. *J. Am. Chem. Soc.* **2007**, *129*, 4306−4322.
(24) Lee, Y. J.; Bingöl, B.; Murakhtina, T.; Sebastiani, D.; Meyer, W. H.; Wegner, G.; Spiess, H. W. High Resolution Solid State NMR Studies of Poly(Vinyl Phosphonicic Acid) Proton Conducting Polymer: Molecular Structure and Proton Dynamics. *J. Phys. Chem. B* **2007**, *111*, 9711−9721.
(25) Lee, Y. J.; Murakhtina, T.; Sebastiani, D.; Spiess, H. W. ^{2}H Solid State NMR of Mobile Protons: It is not always the Simple Way. *J. Am. Chem. Soc.* **2007**, *129*, 12406−12407.
(26) Siwick, B. J.; Bakker, H. J. On the Role ofWater in Intermolecular Proton-Transfer Reactions. *J. Am. Chem. Soc.* **2007**, *129*, 13412−13420.
(27) Ludueña, G. A.; Kühne, T. D.; Sebastiani, D. Mixed Grotthuss and Vehicle Transport Mechanism in Proton Conducting Polymers from ab Initio Molecular Dynamics Simulations. *Chem. Mater.* **2011**, *23*, 1424−1429.
(28) Vilčiauskas, L.; Kreuer, K.-D. Comment on "Mixed Grotthuss and Vehicle Transport Mechanism in Proton Conducting Polymers from Ab initio Molecular Dynamics Simulations". *Chem. Mater.* **2011**, *23*, 3377−3378.
(29) Ludueña, G. A.; Kühne, T. D.; Sebastiani, D. Reply to Comment on "Mixed Grotthuss and Vehicle Transport Mechanism in Proton Conducting Polymers from Ab initio Molecular Dynamics Simulations". *Chem. Mater.* **2011**, *23*, 3379−3380.
(30) Shokri, A.; Abedin, A.; Fattahi, A.; Kass, S. R. Effect of Hydrogen Bonds on pK_a Values: Importance of Networking. *J. Am. Chem. Soc.* **2012**, *134*, 10646−10650.
(31) Shokri, A.; Schmidt, J.; Wang, X.-B.; Kass, S. R. Hydrogen Bonded Arrays: The Power of Multiple Hydrogen Bonds. *J. Am. Chem. Soc.* **2012**, *134*, 2094−2099.
(32) Hu, F.; Schmidt-Rohr, K.; Hong, M. NMR Detection of pH-Dependent Histidine−Water Proton Exchange Reveals the Conduction Mechanism of a Transmembrane Proton Channel. *J. Am. Chem. Soc.* **2012**, *134*, 3703−3713.
(33) Umeyama, D.; Horike, S.; Inukai, M.; Itakura, T.; Kitagawa, S. Inherent Proton Conduction in a 2D Coordination Framework. *J. Am. Chem. Soc.* **2012**, *134*, 12780−12785.
(34) Pardo, E.; Train, C.; Gontard, G.; Boubekeur, K.; Fabelo, O.; Liu, H.; Dkhil, B.; Lloret, F.; Nakagawa, K.; Tokoro, H.; Ohkoshi, S.-i.; Verdaguer, M. High Proton Conduction in a Chiral Ferromagnetic Metal-Organic Quartz-like Framework. *J. Am. Chem. Soc.* **2011**, *133*, 15328−15331.
(35) Sadakiyo, M.; Okawa, H.; Shigematsu, A.; Ohba, M.; Yamada, T.; Kitagawa, H. Promotion of Low-Humidity Proton Conduction by Controlling Hydrophilicity in Layered Metal-Organic Frameworks. *J. Am. Chem. Soc.* **2012**, *134*, 5472−5475.
(36) Jorgensen, W. L.; Tirado-Rives, J. The OPLS [Optimized Potentials for Liquid Simulations] Potential Functions for Proteins, Energy Minimizations for Crystals of Cyclic Peptides and Crambin. *J. Am. Chem. Soc.* **1988**, *110*, 1657−1666.
(37) Berendsen, H. J. C.; Postma, J. P. M.; van Gunsteren, W. F.; DiNola, A.; Haak, J. R. Molecular Dynamics with Coupling to an External Bath. *J. Chem. Phys.* **1984**, *81*, 3684−3690.
(38) Bussi, G.; Donadio, D.; Parrinello, M. Canonical Sampling through Velocity Rescaling. *J. Chem. Phys.* **2007**, *126*, 014101.
(39) Hohenberg, P.; Kohn, W. Inhomogeneous Electron Gas. *Phys. Rev.* **1964**, *136*, B864−B871.
(40) Kohn, W.; Sham, L. J. Self-Consistent Equations Including Exchange and Correlation Effects. *Phys. Rev.* **1965**, *140*, A1133−A1138.
(41) Jones, R. O.; Gunnarsson, O. The Density Functional Formalism, Its Applications and Prospects. *Rev. Mod. Phys.* **1989**, *61*, 689−746.
(42) VandeVondele, J.; Hutter, J. An Efficient Orbital Transformation Method for Electronic Structure Calculations. *J. Chem. Phys.* **2003**, *118*, 4365−4369.
(43) Kolafa, J. Time-Reversible Always Stable Predictor-Corrector Method for Molecular Dynamics of Polarizable Molecules. *J. Comput. Chem.* **2004**, *25*, 335−342.
(44) Krack, M. Pseudopotentials for H to Kr Optimized for Gradient-Corrected Exchange-Correlation Functionals. *Theor. Chem. Acc.* **2005**, *114*, 145−152.
(45) VandeVondele, J.; Krack, M.; Mohamed, F.; Parrinello, M.; Chassaing, T.; Hutter, J. QUICKSTEP: Fast and Accurate Density Functional Calculations using a Mixed Gaussian and Plane Waves Approach. *Comput. Phys. Commun.* **2005**, *167*, 103−128.
(46) Becke, A. D. Density-Functional Exchange-Energy Approximation with Correct Asymptotic Behavior. *Phys. Rev. A* **1988**, *38*, 3098−3100.
(47) Lee, C.; Yang, W.; Parr, R. G. Development of the Colle-Salvetti Correlation-Energy Formula into a Functional of the Electron Density. *Phys. Rev. B* **1988**, *37*, 785−789.
(48) Lippert, G.; Hutter, J.; Parrinello, M. A Hybrid Gaussian and PlaneWave Density Functional Scheme. *Mol. Phys.* **1997**, *92*, 477−487.
(49) VandeVondele, J.; Hutter, J. Gaussian Basis Sets for Accurate Calculations on Molecular Systems in Gas and Condensed Phases. *J. Chem. Phys.* **2007**, *127*, 114105.
(50) Hartwigsen, C.; Goedecker, S.; Hutter, J. Relativistic Separable Dual-Space Gaussian Pseudopotentials from H to Rn. *Phys. Rev. B* **1998**, *58*, 3641−3662.
(51) Goedecker, S.; Teter, M.; Hutter, J. Separable Dual-Space Gaussian Pseudopotentials. *Phys. Rev. B* **1996**, *54*, 1703−1710.
(52) Grimme, S. Semiempirical GGA-type Density Functional constructed with a Long-Range Dispersion Correction. *J. Comput. Chem.* **2006**, *27*, 1787−1799.

(53) Schiffmann, C.; Sebastiani, D. Hydrogen Bond Networks: Structure and Dynamics via First-Principles Spectroscopy. *Phys. Status Solidi B* **2012**, *249*, 368−375.